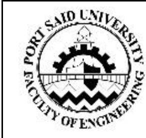

PORT SAID ENGINEERING JOURNAL
Faculty of Engineering - Port Said University
Volume 25 No. 2 September 2021 pp. 165 - 169
-Production Engineering and Mechanical Design-

Design of Micro-Plates Subjected to Residual Stresses in Microelectromechanical Systems (MEMS) Applications

Bahi Bakeer[1], Adel Elsabbagh[2], and Mohammed Hedaya[3]

ABSTRACT

Microelectromechanical Systems (MEMS) devices suffer from reliability problems which affect its performance. Fabrication processes initiate residual stresses that cause stress stiffening and curling. It is shown from the previous research that reducing both stiffening and curling is a challenging issue. Analytical analysis for a fixed-fixed beam is done to determine the factors affecting stiffening in rectangular cross-section beams. A new U-shaped cross-section plate is proposed to decrease both stiffening and curling. The new U-shaped plate is compared with a reference flat plate with the same bending stiffness, length, width, and material properties. To capture plate effects and biaxial residual stress, Finite Element model is developed. Results showed better performance of the U-shaped plate than the flat one. Curling and stiffening reduced by 72 and 42 %, respectively. Stiffness variation with temperature reduced by 43%, stabilizing the operational performance parameters such as pull-in voltage. Moreover, the critical buckling temperature of the U-shaped plate is greater than that of the flat one by 27 ℃, extending the operational temperature range of the plate. The fundamental natural frequency increased by 33%, due to the lower mass of the U-shaped plate. In general, high switching time is considered as another reliability problem in MEMS devices. The increase in fundamental natural frequency for U-shaped plate expects to reduce the switching time. The concept of U-shape plate can be used in many MEMS applications such as resonators, Radio-frequency (RF) switches, pressure sensors, and micromirrors in order to improve the reliability of these devices.

Keywords: Curling, Microelectromechanical systems (MEMS), stiffening, stress gradient.

1. INTRODUCTION

Microelectromechanical systems (MEMS) commercial emergence in the 1970s [1]. MEMS are used in diverse applications such as pressure sensors, accelerometers, mass flow sensors, micropumps, Radio-frequency (RF) switches…. etc. MEMS devices showed many advantages over the large-scale counterparts. The main advantages are their lower cost and higher accuracy. These microsystems consist of mechanical elements such as beams and plates. The fabrication processes initiate plane direction due to the stress gradient across the thickness. Stress stiffening is the increase in stiffness due to in-plane residual tension stress in axially restrained beams and plates. Stress stiffening increases the pull-in voltage needed to actuate MEMS beams or plates.

A lot of research is done on the mechanical design of MEMS. Cantilever beam curls easily and the non-symmetric orientation of the beam affects its performance [1]. Goldsmith et al. [2] designed a fixed-fixed beam. This design is significantly fixed the performance problems of the cantilever beam, but it suffers from stress stiffening due to the in-plane tension stress. Peroulis et al. [3] designed a rectangular plate anchored via four cantilever springs. They proposed two methods to reduce curling. The first method is based on using different configurations of spring structure. The second method is to use larger thickness of the rectangular plate. Both methods reduce curling, but its value still significant. Nieminen et al. [4] also used fixed-fixed beams and studied the effect of temperature change on the pull-in voltage. They found that the pull-in voltage is increased with decreasing temperature, which affects the reliability of the device. Nieminen et al. [1] proposed a square plate design with linear slits to decrease stiffening. This design is highly affected by stress gradient. Reines et al.[5], [6] designed a circular switch with arced shape slits resembling those in Nieminen et al. [1]switch. However, reducing curling led to an increase in stiffening and vice versa. Goldsmith et al. [7] used a different approach to solve this problem. They returned to the standard fixed-fixed beam but with changing the beam material to Molybdenum to match the coefficient of thermal expansion between the beam and the substrate. But on the other hand, Molybdenum has higher thermal and electrical resistance than other metallic counterparts as

[1]*Teaching Assistant, Design and Production Engineering Department, Faculty of Engineering, Ain Shams University, Cairo, Egypt, email: bahi.bakeer@eng.asu.edu.eg, Corresponding author*

[2]*Professor, Design and Production Engineering Department, Faculty of Engineering, Ain Shams University, Cairo, Egypt, email: aelsabbagh@eng.asu.edu.eg*

[3]*Associate Professor, Design and Production Engineering Department, Faculty of Engineering, Ain Shams University, Cairo, Egypt, email: mohammed_hedaya@eng.asu.edu.eg*

Received: 24-12-2020, Accepted: 09-02-2021
DOI :10.21608/PSERJ.2021.54511.1084

Aluminum and Gold which affects the performance of the device. Mahameed and Rebiez [8] made a new design of thermal buckle beam design similar to Chevron thermal actuator. The movable electrode plate is suspended by several beams. The beams are inclined in the plane of the movable electrode, when temperature changed, thermal expansion or contraction induces in-plane displacement to the plate, this release thermal and intrinsic stresses. To decrease out of plane deflection due to stress gradient, thickness is large compared to width. This large needed thickness makes this design difficult to be achieved by standard thin film processes, so electroplating is used.

Philippine et al. [9] used 2D topology optimization tool to systematically generate designs aim to solve stress stiffening and curling problems. The anchoring locations are as in the design of Reines et al. [5], [6]. They made four formulations and compared the results of these formulations with Reines et al. design. The four formulations are (1) minimize compliance, (2) minimize curling, (3) minimize stress stiffening, (4) minimize stress stiffening with constraint on curling. The same adverse problem was found, the design of minimum curling (formulation 2) has large stress stiffening, and the designs of minimum stress stiffening showed a large value of deflection due to stress gradient. Demirel et al.[10] designed a plate with folded cantilever beam springs to reduce in plane stresses. Bansal et el. used a frame as a reinforcement to a plate for curling reduction[11].

This paper proposes a new design to reduce both stiffening and curling. Analytical investigation is presented in the next section to study the factors affecting stiffening. U- shaped section design is studied. To capture the plate effects, a Finite Element model is developed.

2. ANALYTICAL ANALYSIS

2.1. Exact Solution of Fixed-Fixed Beam Subjected to Axial Tensile Force

Consider a fixed-fixed beam with length L subjected to an axial tensile force P and a transverse concentrated force Q at its mid-length as shown in Figure 1. The beam is split into two cantilever beams as shown in, the left cantilever with $x-z$ axes, and the right cantilever with $\eta - z$ axes.

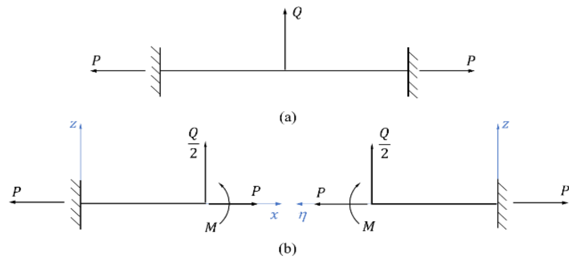

Figure 1: a) fixed-fixed beam subjected to axial tension force P and out of plane force Q at mid-length, b) the fixed-fixed beam is split into two cantilever beams

The governing differential equation of the deflection shape of the beam [12]

$$EI\frac{d^4w}{dx^4} - P\frac{d^2w}{dx^2} = q \tag{1}$$

where E is the elasticity modulus, I is second moment of area, w is the transverse deflection and q is the distributed force per unit length which is zero in our case. For the left cantilever, the solution this differential equation is

$$w(x) = a_1\cosh(\beta x) + a_2\sinh(\beta x) + a_3x + a_4 \tag{2}$$

where a_1, a_2,a_3, and a_4 are constants, and β equals $\sqrt{\frac{P}{EI}}$. Applying boundary conditions

$$w\,(0)\ = 0 \tag{3}$$

$$\frac{dw}{dx}(0) = 0 \tag{4}$$

This gives relations between the constants

$$a_4 = -a_1 \tag{5}$$

$$a_3 = -a_2\beta \tag{6}$$

After substitution in (1), the equation becomes

$$w(x) = a_1[\cosh(\beta x) - 1] + a_2[\sinh(\beta x) - \beta x] \tag{7}$$

The same equation for the right cantilever, but with other constants

$$w(\eta) = a_1^*[\cosh(\beta\eta) - 1] + a_2^*[\sinh(\beta\eta) - \beta\eta] \tag{8}$$

where $\eta = L - x$. Applying compatibility equations at the junction between left and right cantilevers. The deflections and the slopes at the free end of the left and right cantilevers are the same

$$w_1 = w_2 \tag{9}$$

$$\frac{dw_1}{dx} = -\frac{dw_2}{d\eta} \tag{10}$$

where w_1 and w_2 are the deflections at the free ends of the left and right cantilevers, respectively. Considering equilibrium equations in the vicinity of the junction. Isolate a small element near the applied load Q. Applying moment and force equilibrium equations

$$\frac{d^2w_1}{dx^2} = \frac{d^2w_2}{d\eta} \tag{11}$$

$$V_1 + P\frac{dw_1}{dx} = V_2 + P\frac{dw_2}{dx} + Q \tag{12}$$

where V is the shear force. The force equilibrium equation becomes

$$-EI\frac{d^3w_1}{dx^3} - EI\frac{d^3w_2}{d\eta^3} = Q \tag{13}$$

Solving compatibility and equilibrium equations, the stiffness at mid-length of the beam equals to

$$k = \frac{16EIB^3}{L^3}\left[\frac{\sinh(B)}{2 - 2\cosh(B) + B\sinh(B)}\right] \tag{14}$$

where B is a dimensionless variable equals $\frac{L}{2}\sqrt{\frac{P}{EI}}$.

It is difficult to understand the factors affects stiffness from this exact formula, to get a better understanding, Equation (14) is expressed using Taylor expansion as

$$k = \frac{16EI}{L^3}\left(12 + \frac{6}{5}B^2 - \frac{B^4}{700} + \frac{B^6}{63000} \dots\dots\right) \tag{15}$$

Neglecting higher order terms, the linearized model stiffness is

$$k = \frac{192EI}{L^3} + \frac{4.8P}{L} \tag{16}$$

For rectangular cross-section with width W and thickness T, and subjected to residual stress σ_{res} the stiffness is

$$k = \frac{16EWT^3}{L^3} + \frac{4.8\sigma_{res}WT}{L} \tag{17}$$

The first term is the bending stiffness for fixed-fixed beam without applying axial force k_1. The second one is the increase in stiffness due to axial force k_2. For micro-beams and plates, reduction of stiffening ratio k_2/k_1 is desired to lessen the change in the actuation voltage due to the residual axial stress. After the simplification of the analytical model, factors affecting stiffening are obvious. For the same beam material and length, reducing stiffening ratio for rectangular cross-section can be achieved by increasing thickness. Unfortunately, increasing thickness is not suitable for surface micromachining fabrication processes. Therefore, trying new cross-sections other than rectangular one, may be beneficial to reduce stiffening. U-shaped cross section is proposed. The details of the design are shown in the next section.

2.2. Plate Design

Figure 2 shows a diagram of the prismatic U-shaped plate and its dimensions. The plate consists of a base layer of thickness T and two reinforcements at the ends each with width $10 \times T$. Reinforcement height is chosen to be $2 \times T$ in order to make the plate fabrication suitable to surface micromachining processes. For the sake of comparison, the overall length and width are the same of that of a reference flat plate and equal to 250 and 150 μm, respectively. The thickness of the flat reference plate is 3 μm. In order to make a reasonable comparison, the stiffness k_1 of the U-shaped plate is kept the same as the flat reference one. This is achieved by manipulating the thickness of the base layer T until reaching k_1 of the flat plate.

The plate material is Gold with Elasticity modulus E = 45 GPa and Poisson's ratio ν = 0.44.

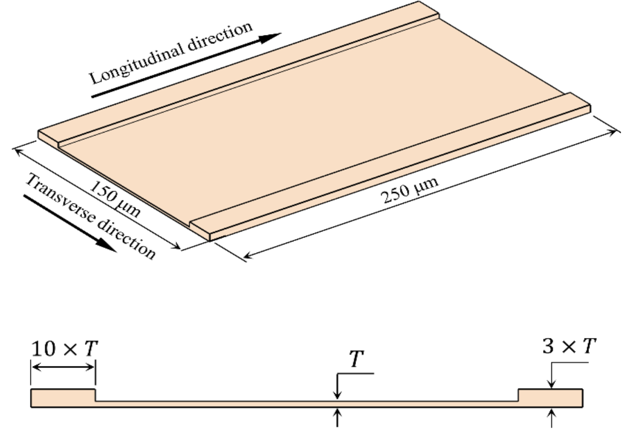

Figure 2: U-shaped plate diagram with dimensions

Beam model stated in the last section cannot capture plate behavior and the biaxial residual stresses. Thus, Finite element (FE) model is developed. The details of the FE model are elaborated in the next section.

3. FINITE ELEMENT (FE) MODEL OF U-SHAPED PLATE

The evaluation of the performance of the U-Shaped plate is done by a 3D FE model which is developed using commercial software COMSOL Multiphysics. Curling, stiffening, natural frequencies, and mode shapes are simulated. The details of these computations are elaborated in the following subsections.

3.1. Curling and Stiffening

Curling is computed by applying the variable stress across the plate thickness. The applied stress gradient equals to 10 $\mathbf{MPa/\mu m}$. The difference between maximum and minimum deflections of the whole plate is considered as the value of curling.

The plate is meshed by rectangular prism elements. The maximum element size is 5 . The actuation area $\boldsymbol{A_{ac}}$ which is the middle third of the plate is subjected to a pressure $\boldsymbol{p}$. The effective stiffness of the plate is calculated as

$$k = \frac{p\,A_{ac}}{w_c} \tag{18}$$

The stiffness $\boldsymbol{k_1}$ is calculated by applying a pressure $\boldsymbol{p}$

to the actuation area. In order to ignore the non-linear effects, a small value of $\boldsymbol{p}$ equals to 10 $\mathbf{N/m^2}$ is applied. To calculate $\boldsymbol{k_2}$, the total stiffness is calculated after applying a biaxial stress of 60 **MPa**. In addition, the geometric non-linearity is taken into consideration in the FE model to consider the coupling between the out of plane deflection and the in-plane stress. Thus, the stiffening ratio $\boldsymbol{k_2/k_1}$ can be calculated.

3.2. Natural Frequencies

Natural frequencies and mode shapes are important performance parameters in MEMS devices. In addition, natural frequency is inversely proportional to the switching time. High switching time is one of the main drawbacks of MEMS devices as radiofrequency switch. The first five natural frequencies and their mode shapes are computed for both flat and U-shaped plates. Natural frequencies simulations are done before and after applying the residual stress.

4. RESULTS AND DISCUSSION

4.1. Curling and Stiffening

The stiffness k_1 of the flat plate equals to 254 N/m. The value of T required for the U-shaped plate to give the same stiffness is 1.75 μm. The same stiffness k_1 is achieved with lower thickness.

Significant reduction in curling and stiffening is found in the new U-shaped plate. Curling is decreased from 352 nm for the flat plate to 73 nm for the U-shaped plate, i.e. a reduction of more than 72 % is achieved. This is due to the consolidation action of the reinforcements at the ends of the plate.

The stiffening ratio k_2/k_1 of the flat and the U-shaped plate are 1.48 and 0.85, respectively. The reason of this stiffening ratio reduction is attributed to the decrease of the cross-sectional area and thus, the decrease in the value of the biaxial force.

4.2. Effect of Operating Temperature on Stiffness

It is desirable to minimize the change in stiffness due to the change in operating temperature for a reliable MEMS device performance. This can positively stabilize other important parameters such as pull-in voltage. Figure 3 shows the change of the total stiffness with temperature for flat and U-shaped plate. the relation is linear related to the axial force as in equation (16). The reduction in stiffness for every 1 ℃ increase in operating temperature for flat and U-shaped plates are 7.2 and 4.1 N/m℃. Thus, U-shaped plate is more stable and reliable. In addition, critical buckling temperature for the U-shaped plate is higher than the flat one by 27 ℃ .

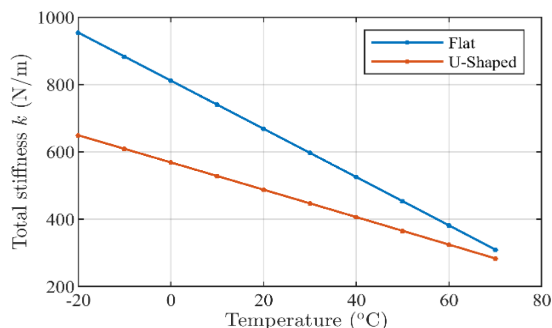

Figure 3: Total stiffness versus operating temperature for both flat and U-shaped plates

4.3. Natural Frequencies

Although both flat and U-shaped plates have the same stiffness k_1, the values of the frequencies are different. The fundamental natural frequencies of the flat and U-shaped plates are 82 and 109 kHz, respectively. This is attributed to the lower mass of the U-shaped plate. Natural frequency is inversely proportional to the switching time [13]. This means that U-shaped plate have another advantage which is lower switching time. Lower switching time is needed in some applications as RF switches. After applying the residual stresses, the values of the fundamental natural frequencies changed to 148 and 153 kHz for flat and U-shaped plates. The total stiffness of the flat plate after applying the residual stresses is about 1.35 of the U-shaped one. This increases the fundamental natural frequency of the flat plate. But the increase is minor due to the lower mass of the U-shaped plate as mentioned before.

Figure 4 shows the first five mode shapes of flat and U-shaped plates. The first two mode shapes are similar in both cases. Thereafter, some modes are delayed, and some came earlier. This can be interpreted by the stiffer behavior of the U-shaped plate resisting bending along the length.

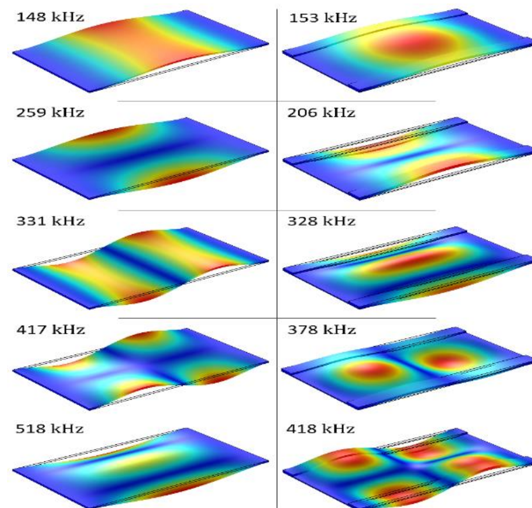

Figure 4: First five mode shapes with their natural frequencies for a) flat and, b) U-shaped plates

5. CONCLUSIONS

This work proposes a solution for the reliability problems related to residual stresses of MEMS devices. To reduce stiffening of beams with rectangular cross-sections, thickness must be increased. Increasing thickness may be not suitable surface micromachining fabrication processes. Thus, plate design with U-shaped cross-section is proposed. Results show better performance of the U-shaped plate than the flat one. Curling and stiffening reduced by 72 and 42 %, respectively. Stiffness change with temperature reduced, thus, stabilizing the operational performance parameters such as pull-in voltage. Moreover, the critical buckling temperature of the U-shaped plate is greater than that of the flat one, extending the operational temperature range of the plate. The fundamental natural frequency increased due to the lower mass of the U-shaped plate. New cross-sections other than U- shaped one can proposed for future work.

Credit Authorship Contribution Statement:

Bahi Bakeer: analytical analysis, Finite Element simulations, writing. Adel Elsabbagh: guidance, review and editing. Mohammed Hedaya: original idea, analytical analysis, review and editing.

Declaration of competing Interest

The authors declare that they have no known competing financial interests or personal relationships that could have appeared to influence the work reported in this paper.

References

[1] H. Nieminen, V. Ermolov, S. Silanto, K. Nybergh, and T. Ryhänen, “Design of a temperature-stable RF MEM capacitor,” *J. Microelectromechanical Syst.*, vol. 13, no. 5, pp. 705–714, 2004, doi: 10.1109/JMEMS.2004.832192.

[2] C. L. Goldsmith, Z. Yao, S. Eshelman, and D. Denniston, “Performance of Low-Loss RF MEMS Capacitive Switches,” *IEEE Microw. Guid. Wave Lett.*, vol. 8, no. 8, pp. 269–271, 1998, doi: 10.1109/75.704410.

[3] D. Peroulis, S. P. Pacheco, K. Sarabandi, and L. P. B. Katehi, “Alleviating the Adverse Effects of Residual Stress in RF MEMS Switches,” 2001.

[4] H. Nieminen, V. Ermolov, K. Nybergh, S. Silanto, and T. Ryhänen, “Microelectromechanical capacitors for RF applications,” *J. Micromechanics Microengineering*, vol. 12, no. 2, pp. 177–186, 2002.

[5] I. Reines, B. Pillans, and G. M. Rebeiz, “A stress-tolerant temperature-stable RF MEMS switched capacitor,” in *Proceedings of the IEEE International Conference on Micro Electro Mechanical Systems*, 2009, pp. 880–883.

[6] I. Reines, B. Pillans, and G. M. Rebeiz, “Thin-film aluminum RF MEMS switched capacitors with stress tolerance and temperature stability,” *J. Microelectromechanical Syst.*, vol. 20, no. 1, pp. 193–203, 2011, doi: 10.1109/JMEMS.2010.2090505.

[7] C. Goldsmith *et al.*, “Performance of molybdenum as a mechanical membrane for RF MEMS switches,” in *IEEE MTT-S International Microwave Symposium Digest*, 2009, pp. 1229–1232, doi: 10.1109/MWSYM.2009.5165925.

[8] R. Mahameed and G. M. Rebeiz, “A high-power temperature-stable electrostatic RF MEMS capacitive switch based on a thermal buckle-beam design,” *J. Microelectromechanical Syst.*, vol. 19, no. 4, pp. 816–826, 2010, doi: 10.1109/JMEMS.2010.2049475.

[9] M. A. Philippine, O. Sigmund, G. M. Rebeiz, and T. W. Kenny, “Topology Optimization of Stressed Capacitive RF MEMS Switches,” *J. Microelectromechanical Syst.*, vol. 22, no. 1, pp. 206–215, 2013.

[10] K. Demirel, E. Yazgan, S. Demir, and T. Akin, “A New Temperature-Tolerant RF MEMS Switch Structure Design and Fabrication for Ka-Band Applications,” *J. Microelectromechanical Syst.*, vol. 25, no. 1, pp. 60–68, 2016, doi: 10.1109/JMEMS.2015.2485659.

[11] D. Bansal *et al.*, “Low voltage driven RF MEMS capacitive switch using reinforcement for reduced buckling,” *J. Micromechanics Microengineering*, vol. 27, no. 2, p. 024001, 2017, doi: 10.1088/1361-6439/aa4ea1.

[12] J. F. Doyle, *Static and Dynamic Analysis of Structures*. Springer, 1991.

[13] G. M. Rebeiz, *RF MEMS, Theory, Design, and Technology*. NewYork: Wiley, 2003.